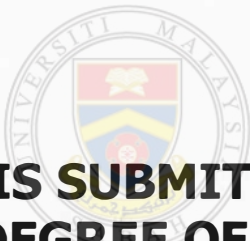


**PIEZOELECTRIC BASED CONCRETE  
STRENGTH MONITORING MODEL**

**KWONG KOK ZEE**



UMS

**THESIS SUBMITTED IN FULFILLMENT FOR  
THE DEGREE OF DOCTOR OF PHILOSOPHY**

**FACULTY OF ENGINEERING  
UNIVERSITI MALAYSIA SABAH  
2018**

# UNIVERSITI MALAYSIA SABAH

## BORANG PENGESAHAN STATUS TESIS

JUDUL: **PIEZOELECTRIC BASED CONCRETE STRENGTH MONITORING MODEL**

IJAZAH: **DOCTOR OF PHILOSOPHY (CIVIL ENGINEERING)**

Saya **KWONG KOK ZEE**, Sesi **2013 – 2014**, mengaku membenarkan tesis Sarjana ini disimpan di Perpustakaan Universiti Malaysia Sabah dengan syarat – syarat kegunaan seperti berikut:

1. Tesis ini adalah hak milik Universiti Malaysia Sabah.
2. Perpustakaan Universiti Malaysia Sabah dibenarkan membuat salinan untuk tujuan pengajian sahaja.
3. Perpustakaan dibenarkan membuat salinan tesis ini sebagai bahan pertukaran antara institusi pengajian tinggi.
4. Sila tandakan (/):

SULIT

(Mengandungi maklumat yang berdarjah keselamatan atau kepentingan Malaysia seperti yang termaktub di dalam AKTA RAHSIA 1972)

TERHAD

(Mengandungi maklumat TERHAD yang telah ditentukan oleh organisasi/badan di mana penyelidikan dijalankan)

TIDAK TERHAD

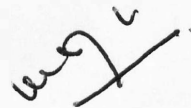


**KWONG KOK ZEE**  
**DK 1311002T**

Tarikh: 30 September 2017

Disahkan Oleh,

NURULAIN BINTI ISMAIL  
PUSTAKAWA KAMAL  
UNIVERSITI MALAYSIA SABAH  
(Tandatangan Pustakawan)



(Prof. Madya Dr. Willey Liew Yun Hsien)  
Penyelia Utama

# DECLARATION

I hereby declare that the material in this thesis is my own except for quotations, excerpts, equations, summaries and references, which have been duly acknowledged.

26 July 2017



---

Kwong Kok Zee  
DK 1311002T



UMS  
UNIVERSITI MALAYSIA SABAH

# CERTIFICATION

NAME : KWONG KOK ZEE  
MATRIC NO. : DK 1311002T  
TITLE : PIEZOELECTRIC BASED CONCRETE STRENGTH  
MONITORING MODEL  
DEGREE : DOCTOR OF PHILOSOPHY (CIVIL ENGINEERING)  
VIVA DATE : 26 JULY 2017

## CERTIFIED BY

### 1. MAIN SUPERVISOR

Prof. Madya Dr. Willey Liew Yun Hsien

Signature



UMS  
UNIVERSITI MALAYSIA SABAH

A handwritten signature in black ink, appearing to be 'wly', is written over a horizontal line.

## ACKNOWLEDGEMENTS

I would like to express my deepest appreciation to my supervisor, Assoc. Prof. Dr. Willey Liew Yun Hsien for being generous, caring and understanding to me. Thank you for being very supportive to me.

I would also like to express my highest gratitude to my co-supervisor, Dr. Lim Yee Yan for being patient in guiding me. Thank you for your willingness to take me as your PhD student and believing in me. This thesis would not have been completed without your guidance.

I am also thankful to Prof. Ir. Dr. Abdul Karim Mirasa for encouraging me and supporting me. To my friends, Nelly, Malisa and Lau, thank you for your help in sharing the knowledge in conducting the experiments.

I would also like to thank all the technicians in the Concrete Laboratory, Electric and Electronic Lab and staff at the Faculty of Engineering, for all the support and kind assistance.

Finally, I would like to express my highest appreciate to my wife, Doris. Thank you for always being there for me throughout all the ups and downs of my life. I would like to thank all my family members. Thank you for your love, understanding and supportive to me.

Kwong Kok Zee  
26 July 2017

# ABSTRACT

Concrete strength monitoring, providing information related to the readiness of the structure for service, is crucial to the safety and resource planning in the construction industry. The advent of smart material, namely piezoelectric (Lead Zirconate Titanate, PZT) transducer, has the potential of overcoming some shortcomings of the conventional structural health monitoring (SHM) techniques, which are time-consuming, labor and cost-intensive, requiring bulky equipment and exposing inspectors to the dangerous environment. Despite the superiority of PZT based SHM techniques, studies conducted thus far are non-parametric, qualitative and lab-based in nature, which limits its potential use in real-life application. This is one of the key limitations of the current smart based monitoring technology, which a direct and accurate strength prediction model is unavailable. The lack of physical model and understanding limits their development and potential in real-life applications. In this research, a novel parametric based, semi-analytical model was developed for the surface bonded PZT based wave propagation (WP) technique for strength evaluation of concrete throughout the curing process. Mechanical parameters of the mortar specimen were mathematically derived from the surface wave (R-wave) and pressure wave (P-wave) using elastic wave equations. These parameters were then empirically correlated to the strength. A proof-of-concept strength calibration chart was finally developed using the semi-empirical model. The model was found to be very robust as it could be generalized to account for different water to cement (W/C) ratio. The performance of the WP technique was then compared to the electromechanical impedance (EMI) technique and the conventional techniques, such as the ultrasonic pulse velocity (UPV) and rebound hammer (RH) test. Results showed that the WP technique performed equally well as the conventional counterparts. The proposed technique is also advantageous over the embedded based WP technique and UPV test, in terms of its capability to capture two types of waves for the evaluation of the dynamic modulus of elasticity and Poisson's ratio. Despite promising performance based on lab-based study, various practical issues affecting the real-life application and the reliability of the technique has not been addressed. In this research, a series of experimental studies were performed to investigate the aforementioned problems, in an attempt to reduce the gap between laboratory and real-life application. Some key issues related to the practical application of this technique were identified and studied, including the consistency and repeatability of the sensor electrical signatures, waveform pattern, frequency selection, the effect of varying PZT transducer' spacing, the sizes of PZT transducer, surface roughness of the host structure, the environmental condition and the effects of different coarse aggregates. Such understanding is essential to serve as guidelines for future design optimization of a more effective PZT based WP technique. Results indicated that the performance of the WP technique was reliable and consistent across different specimens, with different sizes and spacing of PZT transducers. A separate study was finally

conducted to verify the applicability of this technique on the heterogeneous concrete specimen. A finite element (FE) model was proposed to have a better understanding of the behaviour of the PZT based WP technique. The finding from the research has patched up the gap between theory and practice of a PZT based monitoring system for concrete strength by using WP technique, which can be a useful tool in real-time concrete strength prediction, optimizing the time of falsework dismantling, at the same time, ensuring the quality of concrete structure, improving its safety as well as bringing huge savings in terms of time and cost to the construction industry.



UMS  
UNIVERSITI MALAYSIA SABAH

# **ABSTRAK**

## **PEMANTAUAN PENGHIDRATAN KONKRIT BERDASARKAN PIEZOELEKTRIK**

Pemantauan kekuatan konkrit memberikan maklumat yang berkaitan dengan kesediaan penggunaan struktur. Ini adalah penting untuk perancangan keselamatan dan sumber dalam industri pembinaan. Kemunculan bahan pintar, iaitu transduser piezoelektrik (Lead zirkonat Titanate, PZT) mempunyai potensi untuk mengatasi beberapa kelemahan teknik konvensional pemantauan kesihatan struktur (SHM) seperti memakan masa, tenaga kerja dan kos intensif, memerlukan peralatan yang besar dan mendedahkan pemeriksa kepada alam sekitar yang berbahaya. Walaupun teknik SHM berasaskan PZT adalah mengunggulkan, kajian yang dijalankan setakat ini adalah bukan parametrik, kualitatif dan dihadkan di makmal sahaja. Ini menghadkan potensinya dalam aplikasi sebenar. Ini merupakan salah satu batasan utama untuk teknologi pemantauan pintar, iaitu ketiadaan model ramalan kekuatan secara langsung dan tepat. Kekurangan model fizikal dan pemahaman menghadkan pembangunan dan potensi mereka dalam aplikasi kehidupan sebenar. Dalam kajian ini, model semi-analisis teknik perambatan gelombang (WP) berdasarkan PZT digunakan untuk penilaian kekuatan konkrit sepanjang proses pengawetan. Parameter mekanik spesimen mortar telah dinilai secara matematik dari gelombang permukaan (R-gelombang) dan gelombang tekanan (P-gelombang) dengan menggunakan formula gelombang elastik. Parameter ini kemudiannya dikaitkan dengan kekuatan secara empirik. Model semi-empirikal dan carta kekuatan penentukuran telah dibangunkan antara halaju R-gelombang dan kekuatan. Model ini didapati sangat berguna kerana ia boleh digunakan dengan mengambil kira nisbah air dengan simen yang berbeza. Prestasi teknik ini kemudiannya dibandingkan dengan teknik galangan elektromekanik (EMI) dan teknik-teknik konvensional, seperti ujian halaju ultrasonik (UPV) dan pemantulan tukul (RH). Hasil kajian ini menunjukkan bahawa prestasi teknik WP adalah sama dengan prestasi teknik-teknik konvensional. Teknik yang dicadangkan juga lebih berfaedah berbanding teknik WP tertanam dan ujian UPV dari segi keupayaannya untuk menguasai dua jenis gelombang untuk penilaian modulus dinamik keanjalan dan nisbah Poisson. Walaupun prestasi teknik WP adalah menjanjikan berdasarkan kajian berasaskan makmal, pelbagai isu-isu praktikal yang memberi kesan kepada aplikasi sebenar dan kebolehpercayaan teknik ini belum lagi ditangani. Dalam kajian ini, satu siri kajian eksperimen telah dijalankan untuk menyiasat masalah yang dinyatakan di atas, dalam usaha untuk mengurangkan jurang antara makmal dan aplikasi sebenar. Beberapa isu utama yang berkaitan dengan permohonan praktikal teknik ini telah dikenal pasti dan dikaji, termasuk konsisten dan kebolehulangan tandatangan elektrik sensor, corak gelombang, pemilihan frekuensi, jarak antara PZT, saiz PZT, kekasaran permukaan struktur, keadaan sekeliling dan kesan agregat kasar. Pemahaman ini



# **ABSTRAK**

## **PEMANTAUAN PENGHIDRATAN KONKRIT BERDASARKAN PIEZOELEKTRIK**

Pemantauan kekuatan konkrit memberikan maklumat yang berkaitan dengan kesediaan penggunaan struktur. Ini adalah penting untuk perancangan keselamatan dan sumber dalam industri pembinaan. Kemunculan bahan pintar, iaitu transduser piezoelektrik (Lead zirkonat Titanate, PZT) mempunyai potensi untuk mengatasi beberapa kelemahan teknik konvensional pemantauan kesihatan struktur (SHM) seperti memakan masa, tenaga kerja dan kos intensif, memerlukan peralatan yang besar dan mendedahkan pemeriksa kepada alam sekitar yang berbahaya. Walaupun teknik SHM berasaskan PZT adalah mengunggulkan, kajian yang dijalankan setakat ini adalah bukan parametrik, kualitatif dan dihadkan di makmal sahaja. Ini menghadkan potensinya dalam aplikasi sebenar. Ini merupakan salah satu batasan utama untuk teknologi pemantauan pintar, iaitu ketiadaan model ramalan kekuatan secara langsung dan tepat. Kekurangan model fizikal dan pemahaman menghadkan pembangunan dan potensi mereka dalam aplikasi kehidupan sebenar. Dalam kajian ini, model semi-analisis teknik perambatan gelombang (WP) berdasarkan PZT digunakan untuk penilaian kekuatan konkrit sepanjang proses pengawetan. Parameter mekanik spesimen mortar telah dinilai secara matematik dari gelombang permukaan (R-gelombang) dan gelombang tekanan (P-gelombang) dengan menggunakan formula gelombang elastik. Parameter ini kemudiannya dikaitkan dengan kekuatan secara empirik. Model semi-empirikal dan carta kekuatan penentukuran telah dibangunkan antara halaju R-gelombang dan kekuatan. Model ini didapati sangat berguna kerana ia boleh digunakan dengan mengambil kira nisbah air dengan simen yang berbeza. Prestasi teknik ini kemudiannya dibandingkan dengan teknik galangan elektromekanik (EMI) dan teknik-teknik konvensional, seperti ujian halaju ultrasonik (UPV) dan pemantulan tukul (RH). Hasil kajian ini menunjukkan bahawa prestasi teknik WP adalah sama dengan prestasi teknik-teknik konvensional. Teknik yang dicadangkan juga lebih berfaedah berbanding teknik WP tertanam dan ujian UPV dari segi keupayaannya untuk menguasai dua jenis gelombang untuk penilaian modulus dinamik keanjalan dan nisbah Poisson. Walaupun prestasi teknik WP adalah menjanjikan berdasarkan kajian berasaskan makmal, pelbagai isu-isu praktikal yang memberi kesan kepada aplikasi sebenar dan kebolehpercayaan teknik ini belum lagi ditangani. Dalam kajian ini, satu siri kajian eksperimen telah dijalankan untuk menyiasat masalah yang dinyatakan di atas, dalam usaha untuk mengurangkan jurang antara makmal dan aplikasi sebenar. Beberapa isu utama yang berkaitan dengan permohonan praktikal teknik ini telah dikenal pasti dan dikaji, termasuk konsisten dan kebolehulangan tandatangan elektrik sensor, corak gelombang, pemilihan frekuensi, jarak antara PZT, saiz PZT, kekasaran permukaan struktur, keadaan sekeliling dan kesan agregat kasar. Pemahaman ini

adalah penting dijadikan sebagai garis panduan untuk pengoptimuman teknik WP yang lebih berkesan pada masa depan. Keputusan kajian ini menunjukkan bahawa prestasi teknik WP ini boleh dipercayai dan konsisten pada spesimen yang berbeza dengan pelbagai jenis saiz dan jarak antara PZT. Akhirnya, satu kajian berasingan telah dijalankan untuk mengesahkan kesesuaian teknik ini pada spesimen konkrit. Model unsur terhingga (FE) dicadangkan untuk mendapatkan pemahaman yang lebih mendalam mengenai teknik perambatan gelombang (WP) berdasarkan PZT. Penyelidikan ini telah mengurangkan jurang antara teori dan amalan sistem pemantauan PZT untuk kekuatan konkrit dengan menggunakan teknik WP, yang boleh menjadi alat yang berguna dalam ramalan kekuatan konkrit masa nyata, mengoptimumkan masa pembukaan acuan, pada masa yang sama, memastikan kualiti struktur konkrit, meningkatkan keselamatan serta membawa penjimatan besar dari segi masa dan kos kepada industri pembinaan.



UMS  
UNIVERSITI MALAYSIA SABAH

# LIST OF CONTENTS

	Pages
<b>TITLE</b>	i
<b>DECLARATION</b>	ii
<b>CERTIFICATION</b>	iii
<b>ACKNOWLEDGEMENTS</b>	iv
<b>ABSTRACT</b>	v
<b><i>ABSTRAK</i></b>	vii
<b>LIST OF CONTENTS</b>	ix
<b>LIST OF TABLES</b>	xv
<b>LIST OF FIGURES</b>	xvii
<b>LIST OF ABBREVIATIONS</b>	xxii
<b>LIST OF SYMBOLS</b>	xxiii
<b>LIST OF APPENDICES</b>	xxvii
<b>CHAPTER 1: INTRODUCTION</b>	<b>1</b>
1.0 Background	1
1.1 Structural Failure During Construction	3
1.2 Structural Health Monitoring (SHM)	6
1.3 Concrete Strength Monitoring	6
1.4 Problem Statement	9
1.5 Research Objectives	9
1.6 Research Originality and Contributions	10
1.7 Thesis Organization	11
<b>CHAPTER 2: LITERATURE REVIEW</b>	<b>13</b>
2.0 Overview of Structural Health Monitoring	13
2.1 Overview of Concrete Strength Monitoring	14
2.2 Concrete Monitoring Techniques	14
2.2.1 Destructive Testing Technique	14
2.2.1 (a) Core Test	15
2.2.1 (b) Compression Test	16

2.2.2	Non-destructive Testing (NDT) Technique	17
2.2.2 (a)	Freshcon System	17
2.2.2 (b)	Ultrasonic Pulse Velocity (UPV) Test	18
2.2.2 (c)	Rebound Hammer (RH) Test	21
2.3	Advent of Smart Materials, Structures and Systems in SHM	23
2.3.1	Background	23
2.3.2	Smart Materials, Structures and Systems	24
2.3.3	Application of Smart Materials in SHM	25
2.4	Piezoelectricity and Piezoelectric Materials	25
2.4.1	Background	25
2.4.2	Fundamentals of Piezoelectric Materials	26
2.4.3	Piezoelectric Constitutive Relations	28
2.4.4	Piezoceramics	32
2.5	Application of Piezoelectric Materials	34
2.5.1	Physical Principles of Electromechanical Impedance (EMI) Technique	35
2.5.2	Application of EMI Technique in SHM	38
2.6	Physical Principles of Wave Propagation (WP) Technique	40
2.6.1	Pressure Wave (P-wave)	42
2.6.2	Shear Wave (S-wave)	43
2.6.3	Surface Wave or Rayleigh Wave (R-wave)	43
2.6.4	Application of WP Technique in SHM	44
2.6.4 (a)	Embedded PZT based WP Technique	44
2.6.4 (b)	Surface bonded PZT based WP technique	46
2.7	Modeling of WP Technique	48
2.8	Practical Consideration Related to Application of WP Technique in SHM	52
2.8.1	Waveform and Frequency Range Selection	53
2.8.2	Excitation Voltage and Signature Acquisition	54
2.8.3	Sensing Range and Optimal Distance of PZT Transducers	54
2.8.4	Consistency and Reliability of PZT Transducer	55
2.9	Critique of the Reviewed Work on Problem Statement	55

<b>CHAPTER 3: DEVELOPMENT OF WP BASED SEMI-ANALYTICAL STRENGTH PREDICTION MODEL</b>	<b>58</b>
3.0 Introduction	58
3.1 Mathematical Model for Dynamic Modulus of Elasticity and Poisson's Ratio Evaluation	59
3.1.1 P-Wave Equation	59
3.1.2 S-Wave Equation	64
3.1.3 R-Wave Equation	64
3.2 Empirical Model for Strength Prediction Model	72
3.3 Concluding and Remarks	74
<b>CHAPTER 4 APPLICABILITY OF WP TECHNIQUE IN PARAMETRIC STRENGTH PREDICTION</b>	<b>76</b>
4.0 Introduction	76
4.1 Methodology	76
4.1.1 Material and Specimens	76
4.1.2 Experimental Setup and Considerations	83
4.1.3 Data Acquisitions and Frequency Selection	85
4.1.4 Time of Flight (TOF) and Wave Velocities	87
4.1.5 TOF Detection by Using Signal Processing (Cross-Correlation)	89
4.2 Results and Discussions	92
4.2.1 TOF and Wave Velocity	94
4.2.1 (a) Consistency of Wave Velocity	94
4.2.1 (b) Wave Velocity as Strength Indicator	97
4.2.2 Amplitude	98
4.3 Determination of Dynamic Modulus and Poisson's Ratio	99
4.4 Strength Calibration for WP Technique	102
4.5 Concluding Remarks	106
<b>CHAPTER 5: NON-DESTRUCTIVE CONCRETE STRENGTH EVALUATION USING PIEZOELECTRIC BASED WAVE PROPAGATION TECHNIQUE – A COMPARATIVE STUDY</b>	<b>107</b>
5.0 Introduction	107

5.1	Methodology	107
5.1.1	Experimental Setup and Considerations	107
5.2	UPV test	109
5.3	RH test	113
5.4	Comparative Study	115
5.5	Comparison with EMI Technique	117
5.6	Concluding Remarks	119
<b>CHAPTER 6: PRACTICAL ISSUES RELATED TO THE APPLICATION OF PZT BASED WAVE PROPAGATION TECHNIQUE IN MONITORING OF MORTAR CURING</b>		<b>121</b>
6.0	Introduction	121
6.1	Methodology	121
6.1.1	Experimental Setup and Considerations	121
6.2	Results and Discussions	124
6.2.1	Pattern of Actuator Waveform	124
6.2.2	Effect of Varying Frequency	125
6.2.3	Consistency and Repeatability of PZT Transducer Signal Electrical Signatures	127
6.2.3 (a)	Consistency of Electrical Signatures	127
6.2.3 (b)	Repeatability of Electrical Signatures	130
6.2.4	Optimum Transducer Spacing	131
6.2.4 (a)	Maximum Allowable Spacing	132
6.2.4 (b)	Minimum Allowable Spacing and Near Field Effect	133
6.2.5	Size Effect	134
6.2.5 (a)	Amplitude of Sensor Electrical Signature	134
6.2.5 (b)	Wave Velocity	136
6.2.6	Effect of Surface Roughness	138
6.2.7	Effect of Environmental Condition	141
6.2.8	Effect of Coarse Aggregate	144
6.3	Concluding Remarks	147

<b>CHAPTER 7: FINITE ELEMENT MODELING OF PZT BASED WAVE PROPAGATION TECHNIQUE ON CONCRETE STRUCTURE</b>	149
7.0 Background	149
7.1 Review on FE Modeling of PZT – Structure Interaction	149
7.2 Coupled Field FE Modeling and Analysis	150
7.2.1 Principle of Modeling	151
7.3 Modeling of Concrete Beam	153
7.4 Convergence of Solution	157
7.5 Experimental Verification	159
7.6 FEM Parametric Study on PZT-Structure Interaction	161
7.6.1 Dynamic Modulus of Elasticity	161
7.6.2 Poisson’s Ratio	164
7.6.3 Structural Damping	166
7.6.4 Actuation Waveform	168
7.6.5 Frequency Selection	169
7.7 Concluding Remarks	171
<b>CHAPTER 8: CONCLUSIONS AND RECOMMENDATIONS FOR FUTURE WORKS</b>	173
8.0 Review of Objectives	173
8.1 Research Conclusions and Contributions	174
8.1.1 Semi-analytical Parametric Strength Prediction Model	174
8.1.2 Comparison with EMI Technique	174
8.1.3 Comparison with Conventional SHM Technique	174
8.1.4 Repeatability and Consistency of the Electrical Signatures Acquired from PZT Transducer	175
8.1.5 Effect of Environmental Condition	175
8.1.6 Frequency Selection on Actuation	175
8.1.7 Effect of Varying PZT Transducer’ Spacing	175
8.1.8 Effect of Different Sizes of PZT Transducer	175
8.1.9 Effect of Surface Roughness of Host Structure	176
8.1.10 Types of Actuating Waveform	176
8.1.11 Effects of Coarse Aggregates	176

8.1.12	Numerical Simulation of the PZT-structure Interaction of the WP Technique	176
8.2	Recommendations for Future Works	177
8.2.1	Surface Roughness Index of Host Structure	177
8.2.2	Effect of Different Course Aggregate	177
8.2.3	Effect of Bonding and Long-term Protection of PZT Transducer	177
8.2.4	Effect of Temperature and Humidity	177
8.2.5	Effect of Mixing and Curing Condition	178
8.2.6	Other Practical Issues Related to Applications of WP Technique	178
8.2.7	FE Modeling of WP Technique	178
8.2.8	Integrated Use of Smart Materials in SHM	179
	<b>REFERENCES</b>	180
	<b>APPENDICES</b>	190



**UMS**  
UNIVERSITI MALAYSIA SABAH



# LIST OF TABLES

	Page
Table 2.1: Smart materials with unique properties	25
Table 2.2: Typical properties of PZT	33
Table 4.1: Material properties of PIC 151	81
Table 4.2: P-wave and R-wave velocities of mortar specimens	96
Table 4.3: Relationship between curing time, wave velocity, dynamic modulus of elasticity, Poisson's ratio and mortar strength at 120 kHz	100
Table 4.4: Relationship between curing time, predicted mortar strength, average predicted strength, standard deviation and average compression cube test	105
Table 5.1: Wave velocity of UPV and dynamic modulus for L Series and H Series	111
Table 5.2: Predicted strength by UPV test	112
Table 5.3: Mortar strength predicted from RH test	114
Table 5.4: Predicted strength by various testing techniques	116
Table 6.1: Summary of specimens prepared for various experimental studies	123
Table 6.2: P-wave and R-wave velocities of different input waveforms at 28 days	124
Table 6.3: Wave velocities for Specimens CR1 to CR5	129
Table 6.4: Configuration of PZT transducer spacing	131
Table 6.5: P-wave and R-wave amplitude for various PZT transducers spacing on Specimen Sp at 28 days (30 kHz)	132
Table 6.6: Labeling of PZT transducers	134
Table 6.7: Highest peak-to-peak amplitude of sensor signal electrical signature with varying PZT sizes (30 kHz)	136
Table 6.8: Sensor signal amplitude for P-wave and R-wave at 28 days	138
Table 6.9: Physical condition of specimen surface and wave velocities at 28 day	141
Table 6.10: Environmental condition for durability investigation	141

Table 6.11:	Difference in wave velocities (%)	143
Table 6.12:	Relationship between curing time, wave velocity, dynamic modulus of elasticity, strength and predicted strength	145
Table 7.1:	Piezoelectric properties of PIC 151	152
Table 7.2:	Material properties for concrete	153
Table 7.3:	Largest peak-to-peak amplitude of sensor electrical signature for several dynamic modulus of elasticity input in a range of 10 GPa to 40 GPa	163
Table 7.4:	Wave velocities for several dynamic modulus of elasticity input in a range of 10 GPa to 40 GPa	163
Table 7.5:	Largest peak-to-peak amplitude of sensor signal for several Poisson's ratio in a range of 0 to 0.5	165
Table 7.6:	Wave velocities for several Poisson's ratio input in a range of 0 to 0.5	165
Table 7.7:	Wave velocities for varying stiffness damping multipliers ( $1.5 \times 10^{-9}$ to $1.5 \times 10^{-5}$ )	166
Table 7.8:	Largest peak-to-peak amplitude of sensor electrical signature for varying stiffness damping multiplier value ( $1.5 \times 10^{-9}$ to $1.5 \times 10^{-5}$ )	167
Table 7.9:	P-wave and R-wave velocities of different input waveforms at 28 days	169

# LIST OF FIGURES

	Page
Figure 1.1: Formwork and shoring system for staged construction of multi-stories offices	2
Figure 1.2: Production of precast concrete for driven piles on a circulation system in a factory	2
Figure 1.3: Collapse of Skyline Plaza	4
Figure 1.4: Collapse of Willow Island cooling tower	5
Figure 1.5: Concept underlying the use of PZT in SHM	8
Figure 2.1: Cored sample obtained from the concrete structure	16
Figure 2.2: Compression machine for compression test	16
Figure 2.3: The Freshcon system	17
Figure 2.4: UPV test using direct transmission method	19
Figure 2.5: Schematic of UPV instrument	19
Figure 2.6: Typical RH instrument	21
Figure 2.7: Schematic of the RH instrument	22
Figure 2.8: Crystalline structure of a piezoelectric ceramic (a) before polarization and (b) after polarization	27
Figure 2.9: Poling process (1) Prior to polarization polar domains are oriented randomly (2) A very large direct current electric field is used for polarization (3) After the electric field is removed, the remnant polarization remains	27
Figure 2.10: Piezoelectric effect	29
Figure 2.11: A piezoelectric transducer with conventional labels of axes	30
Figure 2.12: Various types and shapes of piezoceramics	33
Figure 2.13: Idealized interactions between a PZT transducer and host structure	35
Figure 2.14: Typical plot of admittance signature versus frequency acquired from PZT transducer surfaced bonded on a concrete beam (100 mm x 100 mm x 500 mm)	36
Figure 2.15: 2-D plane of mechanical waves by vibrating PZT transducer	41

Figure 2.16:	The virtual mechanism of P-wave that travelling in a medium	42
Figure 2.17:	The virtual mechanism of S-wave that travelling in a medium	43
Figure 2.18:	The virtual mechanism of R-wave that travelling on a medium surface	44
Figure 2.19:	Smart aggregate	45
Figure 2.20:	Geometry of the elements	48
Figure 3.1:	Medium undergoing axial vibration: (a) General schematic (b) Infinitesimal axial element (c) Thickness-wise stress distribution	60
Figure 3.2:	Relation between Poisson's ratio and velocity of propagation of P-wave, S-wave and R-wave in a linear elastic homogeneous half-space	71
Figure 3.3:	Typical dynamic modulus versus square root of concrete strength graph showing the constant $k$ value	73
Figure 3.4:	Typical strength calibration chart	74
Figure 4.1:	Weighing of various raw materials	77
Figure 4.2:	Mixing of raw materials	78
Figure 4.3:	Compaction by vibrating table	78
Figure 4.4:	Mortar prisms for H series	79
Figure 4.5:	Mortar cubes for cube test (H series)	79
Figure 4.6:	Compression test equipment	80
Figure 4.7:	PZT transducer	80
Figure 4.8:	PZT transducer with copper wires soldered to the electrode surface	81
Figure 4.9:	Configurations of PZT transducers on typical mortar prism	82
Figure 4.10:	Mortar prisms of H series and L series with surface bonded PZT transducers	82
Figure 4.11:	150 V peak-to-peak Hanning windowed 5-peaks tone burst	84
Figure 4.12:	WP technique experiment setup	85
Figure 4.13:	Actuator-sensor voltage signal against time of H series at different frequencies (Spacing = 120 mm) after 28 days of curing	86

Figure 4.14:	Amplitude versus time of actuator and sensor (scaled) electrical signatures at 120 kHz	88
Figure 4.15:	Distance versus TOF acquired from PZT sensor on H series at 28 days	89
Figure 4.16:	Flowchart in calculating TOF	90
Figure 4.17:	Pictorial illustration of cross correlation of R-wave derived from sensor electrical signatures (scaled)	91
Figure 4.18:	Distribution of cross-correlation of sensing signatures against time	92
Figure 4.19:	Amplitude versus time for actuator-sensor pair of Specimen H1 at 120 kHz after 1 day of curing	93
Figure 4.20:	Distance versus TOF acquired from PZT transducers surface bonded on Specimen L1	95
Figure 4.21:	P-wave velocity (a) and R-wave velocity (b) versus curing time	97
Figure 4.22:	Normalized amplitude of sensor electrical signatures versus curing time	98
Figure 4.23:	Dynamic modulus of elasticity and Poisson's ratio versus curing time for L Series and H Series	101
Figure 4.24:	Relationship between square root of mortar strength and curing time	102
Figure 4.25:	Relationship between dynamic modulus and square root of mortar strength	103
Figure 4.26:	Strength calibration chart for mortar based on WP technique	104
Figure 4.27:	Relationship between UPV (P-wave) and compressive strength of mortar	104
Figure 5.1:	Test equipment	108
Figure 5.2:	Configuration for UPV test and RH test	108
Figure 5.3:	P-wave velocity of UPV	110
Figure 5.4:	Dynamic modulus versus square root of strength based on UPV test	111
Figure 5.5:	Strength calibration chart for mortar based on UPV test	112
Figure 5.6:	RH strength calibration chart	113

Figure 5.7:	Predicted mortar strength versus curing time of various techniques	115
Figure 5.8:	Experiment setup for EMI technique	117
Figure 5.9:	Plot of conductance signatures versus frequency for PZT transducer L1C in the frequency range of 70 – 130 kHz	118
Figure 5.10:	First PZT resonance frequency versus number of curing days	119
Figure 6.1:	Configurations of PZT transducers on typical mortar prism	122
Figure 6.2:	Results of various input waveform for Specimen WF (30 kHz)	125
Figure 6.3:	Sensor electrical signatures with varying frequency range for the specimen Fq (a) 10 kHz to 50 kHz, without amplifier (b) 30 kHz to 120 kHz, with amplifier (Amplitude of 100 kHz and 120 kHz scaled up by 150 times of original output voltage for ease of comparison)	126
Figure 6.4:	Wave velocities versus curing time	128
Figure 6.5:	TOF and velocity for wave of varying PZT spacing acquired from Specimen CR3 (30 kHz)	130
Figure 6.6:	Sensor signature of swapping PZT transducers as actuators and sensors acquired from Specimen CR1 (30 kHz)	131
Figure 6.7:	P-wave and R-wave amplitude for various PZT transducers spacing on Specimen Sp at 28 days (30 kHz)	132
Figure 6.8:	Sensor electrical signatures of range distance between PZT transducers on Specimen Sp at day 28 (30 kHz)	133
Figure 6.9:	Sensor electrical signature with varying PZT sizes (30 kHz) (a) Fixed sensor size (20mm x 20mm x 0.5mm) with varying sizes of actuators (b) Fixed actuator size (20mm x 20mm x 0.5mm) with varying sizes of sensors	135
Figure 6.10:	Wave velocity against curing time (30 kHz)	137
Figure 6.11:	Specimens with different surface roughness	139
Figure 6.12:	Sensors electrical signature at 28 days (30 kHz)	140
Figure 6.13:	Wave velocity versus curing time for different type of surfaces roughness (30 kHz)	140
Figure 6.14:	Specimens in different environmental condition	142

Figure 6.15:	Relationship between dynamic modulus and square root of strength for concrete with different types of aggregate	146
Figure 6.16:	Strength calibration chart on concrete and mortar based on WP technique using R-wave velocity	147
Figure 7.1:	Simulation of WP technique	150
Figure 7.2:	Transmitting boundaries (circled in red) at both ends of concrete beam (top view)	154
Figure 7.3:	FE model for the simulation	155
Figure 7.4:	1 mm element meshing size for the concrete beam and PZT transducers	156
Figure 7.5:	Coupling voltage DOF on PZT transducer	157
Figure 7.6:	Converging of solution at 120 kHz actuation	158
Figure 7.7:	Sensor electrical signature obtained from experiment and FE simulation at 120 kHz actuation	160
Figure 7.8:	FE model of small concrete beam (20 mm x 100 mm x 140 mm) for parametric study	161
Figure 7.9:	FE simulation results for several dynamic modulus of elasticity input in a range of 10 GPa to 40 GPa	162
Figure 7.10:	Wave velocities for several dynamic modulus of elasticity input in a range of 10 GPa to 40 GPa	163
Figure 7.11:	Sensor electrical signature for various input of Poisson's ratio value in a range of 0 to 0.5	164
Figure 7.12:	Wave velocities for several Poisson's ratio input in a range of 0 to 0.5	165
Figure 7.13:	Sensor electrical signature for various input of varying stiffness damping multiplier value, $\beta$ ( $1.5 \times 10^{-9}$ to $1.5 \times 10^{-5}$ )	167
Figure 7.14:	Sensor electrical signature (scaled) of various input waveform	168
Figure 7.15:	FE simulation results of PZT sensor electrical signature (scaled) at various actuating frequencies (30 kHz to 120 kHz)	170

## LIST OF ABBREVIATIONS

<b>ACI</b>	-	American Concrete Institute
<b>ASTM</b>	-	American Society for Testing and Materials
<b>BS</b>	-	British Standard
<b>DOF</b>	-	Degree of Freedom
<b>EMI</b>	-	Electromechanical Impedance
<b>FE</b>	-	Finite Element
<b>FEM</b>	-	Finite Element Method
<b>IEEE</b>	-	The Institute of Electrical and Electronics Engineers
<b>NDE</b>	-	Non-Destructive Evaluation
<b>PWAS</b>	-	Piezoelectric Wafer Active Sensor
<b>PVDF</b>	-	Polyvinylidene Fluoride
<b>PZT</b>	-	Lead Zirconate Titanate
<b>RH</b>	-	Rebound Hammer
<b>RMSD</b>	-	Root Mean Square Deviation
<b>SHM</b>	-	Structural Health Monitoring
<b>TOF</b>	-	Time of Flight
<b>UPV</b>	-	Ultrasonic Pulse Velocity
<b>W/C</b>	-	Water to Cement
<b>WP</b>	-	Wave Propagation